Pterostilbene inhibits lung squamous cell carcinoma growth *in vitro* and *in vivo* by inducing S phase arrest and apoptosis

KOK-TONG TAN[1,2], PING-WEN CHEN[2], SHIMING LI[3], TE-MIN KE[4], SHENG-HAO LIN[5] and CHING-CHIEH YANG[4,6,7]

[1]Department of Surgery, Tungs' Taichung Metro Harbor Hospital, Taichung 433; [2]Institute of Biomedical Science, National Chung-Hsing University, Taichung 402, Taiwan, R.O.C.; [3]Hubei Key Laboratory of Economic Forest Germplasm Improvement and Resources Comprehensive Utilization, Huanggang Normal University, Huanggang, Hubei 438000, P.R. China; [4]Department of Radiation Oncology, Chi-Mei Medical Center, Tainan 710; [5]Division of Chest Medicine, Department of Internal Medicine, Changhua Christian Hospital, Changhua 500; [6]Institute of Biomedical Sciences, National Sun Yat-Sen University, Kaohsiung 804; [7]Department of Pharmacy, Chia-Nan University of Pharmacy and Science, Tainan 717, Taiwan, R.O.C.

Received May 11, 2018; Accepted April 17, 2019

DOI: 10.3892/ol.2019.10499

Abstract. Natural dietary components have become the subject of an increasing amount of interest due to the side effects of anticancer treatment. Pterostilbene, an analog of resveratrol, is primarily found in grapes, and has been suggested to exert antioxidant and anticancer effects in different tumor types. The present study aimed to investigate the antitumor effects and molecular mechanisms of pterostilbene in the human lung squamous cell carcinoma (SqCC) cell line, H520. The results of the present study indicate that pterostilbene significantly reduced cell viability and induced S phase arrest, and that treatment with pterostilbene was associated with the down-regulation of cyclin A and cyclin E, as with the upregulation of p21 and p27 expression in H520 cells. In the apoptosis analysis, pterostilbene induced S phase accumulation and the activation of caspase-3, -8 and -9 in H520 cells, potentially through the activation of extrinsic and intrinsic apoptotic pathways. Additionally, the *in vivo* study demonstrated that pterostilbene effectively inhibited lung SqCC growth in a H520 xenograft model. Given the *in vitro* and *in vivo* antitumor effects of pterostilbene demonstrated in the present study, pterostilbene may serve a novel and effective therapeutic agent to for patients with SqCC.

Correspondence to: Dr Sheng-Hao Lin, Division of Chest Medicine, Department of Internal Medicine, Changhua Christian Hospital, 135 Nanxiao Street, Changhua 500, Taiwan, R.O.C.
E-mail: cmdr.linsh@gmail.com

Dr Ching-Chieh Yang, Department of Radiation Oncology, Chi-Mei Medical Center, 901 Zhonghua Road, Tainan 710, Taiwan, R.O.C.
E-mail: cleanclear0905@gmail.com

Key words: lung squamous cell carcinoma, pterostilbene, cell cycle, apoptosis

Introduction

Lung squamous cell carcinoma (SqCC) is a subtype of non-small cell lung cancer (NSCLC) and represents 25-30% of all lung cancer cases (1). Compared with patients that develop other subtypes, such as adenocarcinoma or large cell carcinoma, patients that develop SqCC are commonly tobacco users or older adults (2). Although the incidence of SqCC has steadily decreased in recent decades, SqCC remains a common malignancy, accounting for >400,000 new cases worldwide each year (3).

Despite being the second most common histological type of NSCLC, the treatment options for lung SqCC remain limited. Surgery is regarded as the primary treatment modality; however, only ~25% of tumors are suitable for potentially curative resection (4). Chemotherapy or a combination of chemotherapy and radiotherapy is often used to improve patient survival (5). However, the treatment results for lung SqCC have remained stagnant over the last decade The 5-year survival rate for lung SqCC is as low as 20%, primarily due to chemotherapy or radiation resistance (6). In addition, treatment-associated side effects often occur, even at usual therapeutic doses (7). Therefore, there is an urgent need to identify novel target therapies, especially those using less-harmful natural materials, for the treatment of lung SqCC.

Pterostilbene (trans-3,5-dimethoxy-4'-hydroxy-stilbene) is a natural dimethyl analog of resveratrol primarily found in grapes and blueberries (8). Pterostilbene has been recently examined as it has been revealed to exert several pharmacological effects similar to those of resveratrol, such as antioxidant, anticancer and anti-inflammatory activities (9). Compared with resveratrol, pterostilbene has greater potential in clinical applications due to its higher bioavailability, including increased oral absorption, better metabolic stability and a higher potential for cellular uptake (10). Previous studies have reported that pterostilbene can inhibit the growth of tumors *in vitro* and *in vivo* in different types of cancer (10,11).

In lung cancer, pterostilbene has been reported as a potent anticancer compound; however, there is limited data presently available regarding the role of pterostilbene in lung SqCC or validation *in vivo* (11). Therefore, the present study aimed to determine the *in vitro* and *in vivo* antitumor activities of pterostilbene in a human lung SqCC cell line. In addition, the possible molecular mechanisms responsible for the anticancer activity of pterostilbene were investigated.

Materials and methods

Cell culture and materials. Although epidermal growth factor receptor (EGFR) mutations serve an important therapeutic role in patients with NSCLC, EGFR mutations are rarely (0-14.6%) identified in lung SqCC (12). Therefore, the present study used EGFR-negative SqCC cell lines (13,14). NCI-H520 and NCI-H226 cells, which are human lung SqCC cell lines, which were purchased from the Food Industry Research and Development Institute (15,16). These cells were maintained in RPMI-1640 supplemented with 10% FBS and an antibiotic-antimycotic agent containing amphotericin B, penicillin and streptomycin. All cell culture reagents were purchased from Invitrogen (Thermo Fisher Scientific, Inc.). The cells were cultured at 37˚C in a humidified incubator with 5% CO_2. The stock dose of pterostilbene (Sigma-Aldrich; Merck KGaA) was 50 mM and was dissolved in a DMSO solution (Sigma-Aldrich; Merck KGaA).

Cell viability assay. H520 cells ($3x10^4$) were seeded into a 24-well plate (Corning, Inc,), and allowed to adhere overnight. The cells were then treated with 1.56, 3.13, 6.25, 12.5 25 and 50 μM pterostilbene for 24 and 48 h. Following 24 and 48 h treatment, cells were incubated with 200 μl 0.5 mg/ml MTT (Sigma-Aldrich; Merck KGaA) for 4 h. Cells treated with 0.1% DMSO were used as the control. The formazan was then dissolved in DMSO, and the optical density (OD) value at 570 nm was measured using an ELISA reader (Tecan Group, Ltd.). The IC50 was calculated by polynomial regression analysis using Microsoft Excel software version 2016 (Microsoft Corporation), and the mean (OD) ± SD for each group of triplicates was calculated.

Propidium iodide (PI) staining. H520 cells ($3x10^5$) were seeded into a 6-well plate (Corning, Inc.), and allowed to adhere overnight in the aforementioned culture conditions. The next day, the cells were treated with 12.5, 25 and 50 μM pterostilbene for 48 h. Following 48 h treatment, cells were collected into a flow tube containing trypsin-EDTA (Gibco; Thermo Fisher Scientific, Inc.) and centrifuged at 1,000 x g for 5 min at 4˚C. Then, the cells were fixed for 16 h in 75% ethanol at -20˚C. The cells were washed using PBS and incubated with 500 μl PBS with 0.1% (v/v) Triton X-100, 100 μg/ml RNase A and 50 μg/ml PI (Sigma-Aldrich; Merck KGaA) for 30 min at room temperature. The sub-G1 population containing apoptotic cells was detected using an Accuri™ C5 flow cytometer (BD Biosciences). Data were further analyzed with the C6 Accuri system software 1.0.264.21 (BD Biosciences).

Annexin-FITC apoptotic assay. H520 cells ($3x10^5$) were seeded into a 6-well plate, and allowed to adhere for 24 h in the aforementioned culture conditions. The cells were then treated with 12.5-50 μM pterostilbene for 48 h. At these time points, the cells were collected into a flow tube containing trypsin-EDTA (Gibco; Thermo Fisher Scientific, Inc.) and centrifuged at 1,000 x g for 5 min at 4˚C. Then, the cells were stained according to the protocol of an Annexin V-FITC apoptosis detection kit (cat. no. 556547; BD Biosciences) for 15 min at room temperature. Finally, the green and red fluorescence of Annexin V/PI were detected with an Accuri™ C5 cytometer in the FL-1 and FL-2 graphs. Data were further analyzed with the C6 Accuri system software 1.0.264.21.

JC-1 staining. H520 cells ($3x10^5$) were seeded into a 6-well plate. The next day, the cells were treated with 12.5-50 M of pterostilbene for 48 h. Following 48 h treatment, the cells were collected into a flow tube containing trypsin-EDTA (Gibco; Thermo Fisher Scientific, Inc.) and centrifuged at 1,000 x g for 5 min at 4˚C. The cells were then stained with 2 μM JC-1 (10 μg/ml; Sigma-Aldrich; Merck KGaA) for 10 min at room temperature. The red and green fluorescence were detected with an Accuri™ C5 cytometer in the FL-1 and FL-2 graphs. Data were further analyzed with the C6 Accuri system software 1.0.264.21.

Western blot analysis. H520 cells ($5x10^5$) were seeded onto a 6-cm plate. The next day, the cells were treated with 12.5-50 μM pterostilbene for 48 h. Following 48 h treatment, the cells were collected into a flow tube containing trypsin-EDTA (Gibco; Thermo Fisher Scientific, Inc.) and centrifuged at 1,000 x g for 5 min at 4˚C. The cells were lysed in RIPA buffer containing 1% protease inhibitor cocktail and 2% PMSF (all from Sigma-Aldrich; Merck KGaA) on ice for 30 min, and the protein concentration in the cell lysates was quantified using a bicinchoninic acid (BCA) protein assay kit (Thermo Fisher Scientific, Inc.). Cytosolic fractions were isolated using the Mitochondria/Cytosol Fraction kit (BioVision, Inc.) according to the manufacturer's instructions and the protein concentration in the cytosolic fraction was quantified using the BCA protein assay kit. The samples were separated using 12% SDS-PAGE and transferred onto a PVDF membrane (EMD Millipore). The membrane was blocked with a blocking buffer containing 5% non-fat milk for 1 h at room temperature and incubated with primary antibodies at 4˚C overnight. The primary antibodies used were as follows: Anti-cyclin A (1:500; cat. no. sc-239, clone BF683; Santa Cruz Biotechnology, Inc.), anti-cyclin E (1:500; cat. no. sc-247, clone HE12; Santa Cruz Biotechnology, Inc.), anti-CDK2 (1:500; cat. no. sc-6248, clone D12; Santa Cruz Biotechnology, Inc.), anti-p21 (1:1,000; cat. no. 2947, clone 12D1; Cell Signaling Technology, Inc.), anti-p27 (1:1,000; cat. no. 3686, clone D69C12; Cell Signaling Technology, Inc.), anti-cytochrome *c* (1:500; cat. no. 4280, clone 136F3; Cell Signaling Technology, Inc.), anti-Bax (1:1,000; cat. no. 5023, clone D2E11; Cell Signaling Technology, Inc.), anti-Bcl-2 (1:1,000 dilution; cat. no. 4223, clone D55G8; Cell Signaling Technology, Inc.) and anti-GAPDH (1:2,000 dilution; cat. no. sc-32233, clone 6C5; Santa Cruz Biotechnologies, Inc.). The next day, membranes were incubated with horseradish peroxidase AffiniPure goat anti-rabbit immunoglobulin G (H+L) (1:2,000; cat. no. 111-035-144; Jackson ImmunoResearch

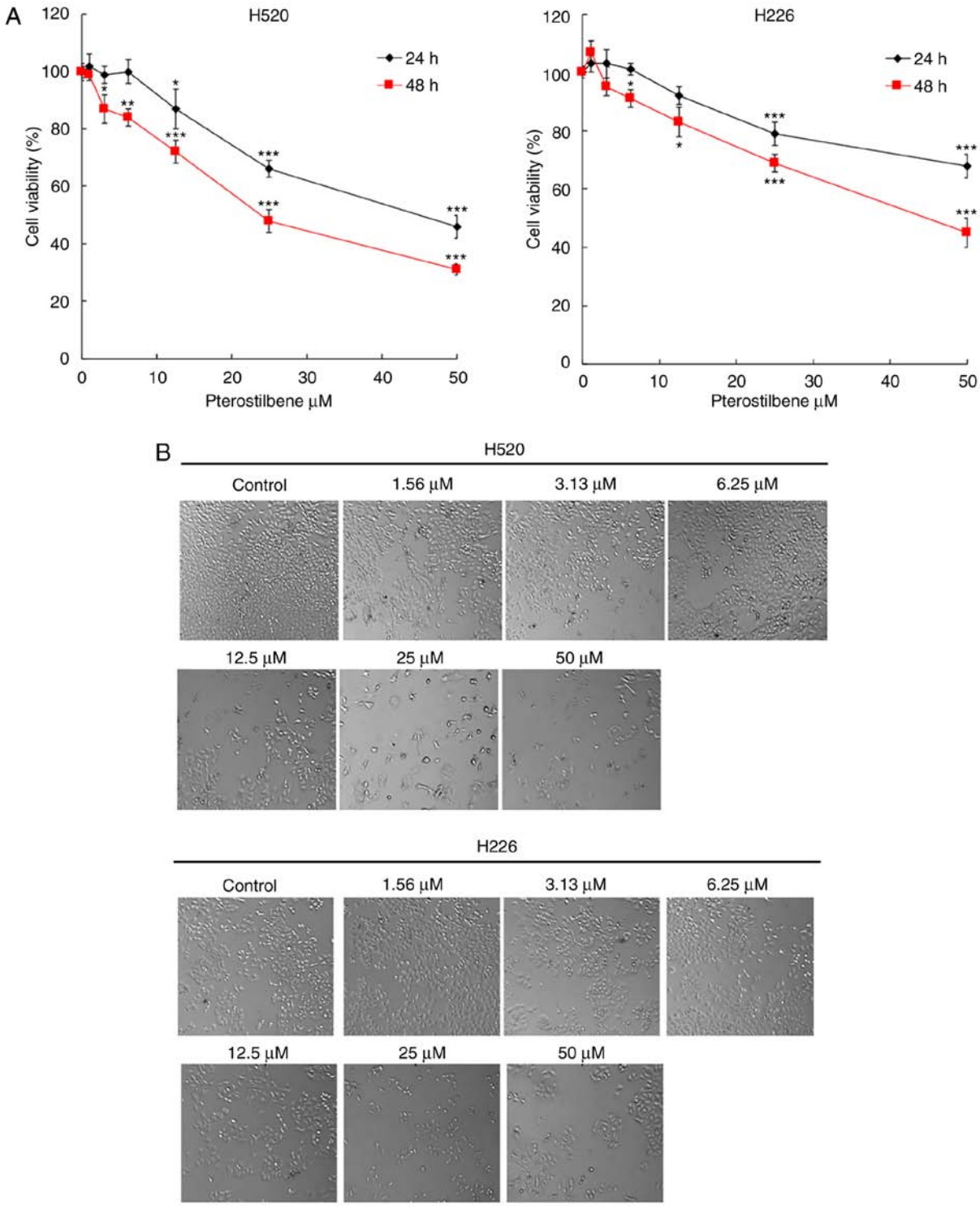

Figure 1. Effect of pterostilbene on the viability of H520 and H226 cells by an MTT assay. (A) Cells were incubated with increasing concentrations of pterostilbene in culture medium for 24 and 48 h. Cell viability was then assessed by an MTT assay. Data presented are the mean ± SD of three independent experiments. *P<0.05, **P<0.01 and ***P<0.001 vs. 0.1% DMSO-treated group. (B) Representative bright-field images of cell morphology (magnification, x100).

Laboratories, Inc.) or horseradish peroxidase AffiniPure Goat Anti-mouse IgG (H+L) (1:2,000; cat. no. 111-035-003; Jackson ImmunoResearch Laboratories, Inc.) at 4˚C overnight. Finally, a Western Lightning® Plus-ECL kit reagent (PerkinElmer, Inc.) was added to the membranes so the immunofluorescence signals could be detected using Hansor Luminescence Image system (Hansor). All bands in the blots were normalized to the level of GAPDH for each lane. The intensity of the bands was quantified using ImageJ 1.47 software for Windows (National Institutes of Health).

Caspase activity assay. H520 cells ($3x10^5$) were seeded into a 6-well plate. The next day, the cells were treated with 12.5-50 M pterostilbene for 48 h. Following 48 h treatment, the cells were collected into a flow tube containing trypsin-EDTA and centrifuged at 1,000 x g for 5 min at 4˚C to remove the

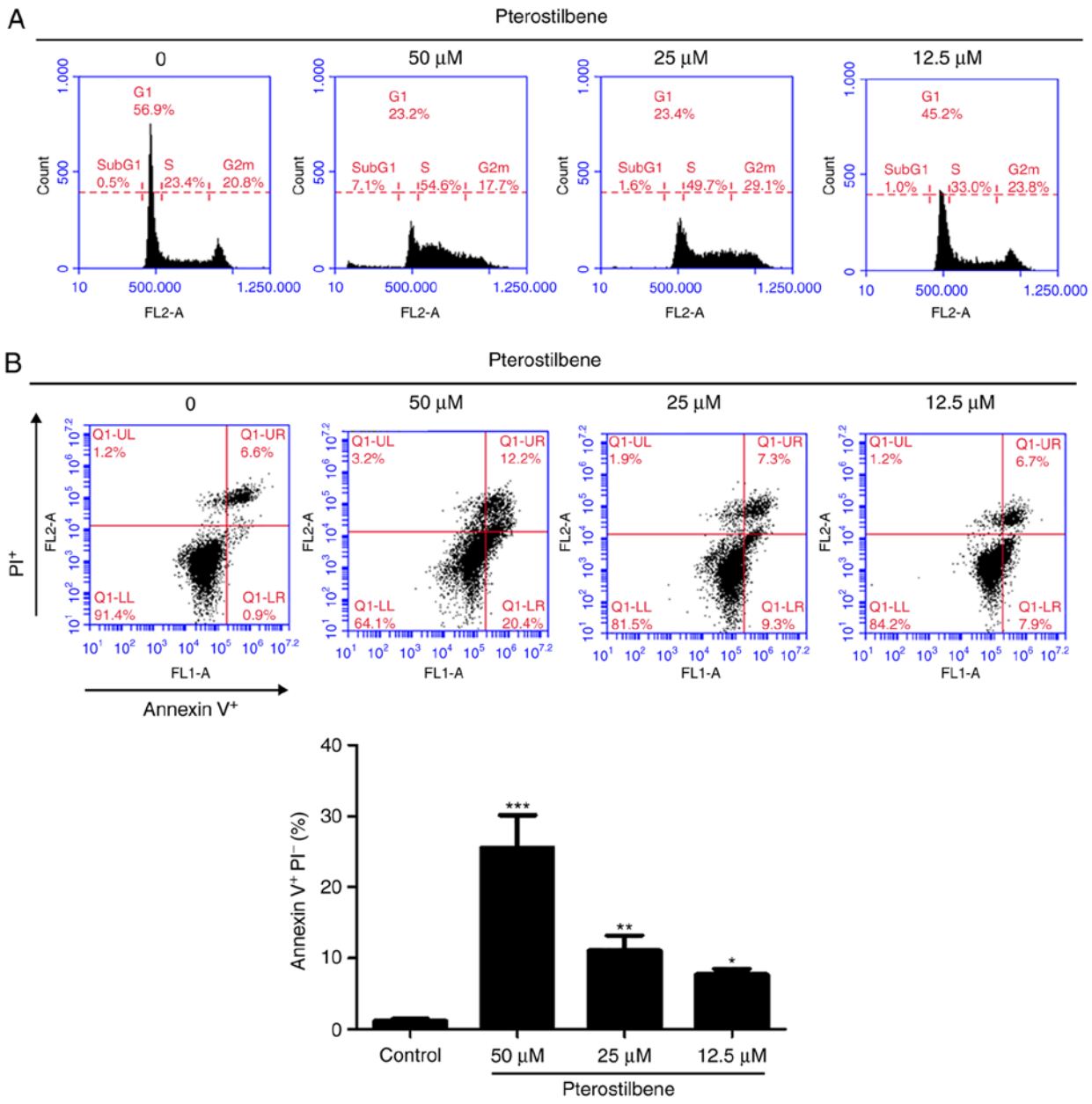

Figure 2. Effects of pterostilbene on cell cycle distribution and apoptosis in H520 cells. (A) Cell cycle analysis of pterostilbene-treated cells. Cells were plated as described in the Materials and methods section with 50, 25 and 12.5 μM pterostilbene for 48 h. Cell cycle distributions were then determined by staining with a PI solution and flow cytometry analysis. Data are representative of three independent experimental repeats. (B) Flow cytometric analysis of Annexin V staining to quantify pterostilbene-induced apoptosis in H520 cells. The dot plots show the results of the treatment of H520 cells with pterostilbene for 48 h. Data are presented as the mean ± SD of triplicate experiments. *P<0.05, **P<0.01 and ***P<0.001 vs. control. PI, propidium iodide.

supernatant. The cells were stained according to the manufacturer's protocol for the CaspGLOW™ fluorescein active caspase-3/-8/-9 staining kit (BioVision, Inc.).

Animal experimentation. Female BALB/c athymic nude mice (18-22 g, 6-week-old) were purchased from the National Laboratory Animal Center (Taipei, Taiwan). A total of 12 animals were categorized into two groups, each comprising 6 mice (n=6). During the whole period of experimental study, animals were housed under standard environmental conditions of temperature and humidity (22±2˚C and 60±10%, respectively) and with 12-h light/dark cycle. All animals had free access to regular rat chow and water ad libitum. All animal experiments were approved by the Institutional Animal Care and Use Committee of National Chung Hsing University.

Tumor xenograft model. H520 cells ($1x10^7$ in 100 μl) was mixed with 0.2 ml of extracellular matrix gel (BD Biosciences) that was inoculated under the skin of the nude mice. When the tumor volume had reached ~10 mm^3, the nude mice (n=6 per cage) were intraperitoneally administered 50 mg/kg pterostilbene or the vehicle control (10% DMSO + 90% glyceryl trioctanoate; Sigma-Aldrich; Merck KGaA) every other day continuously until day 37. On day 38, the nude mice were sacrificed using 30 psi CO_2 for 15-20 sec until cardiac arrest. Subsequently, the tumors were excised from the nude mice, images of the tumors were obtained, the tumors were

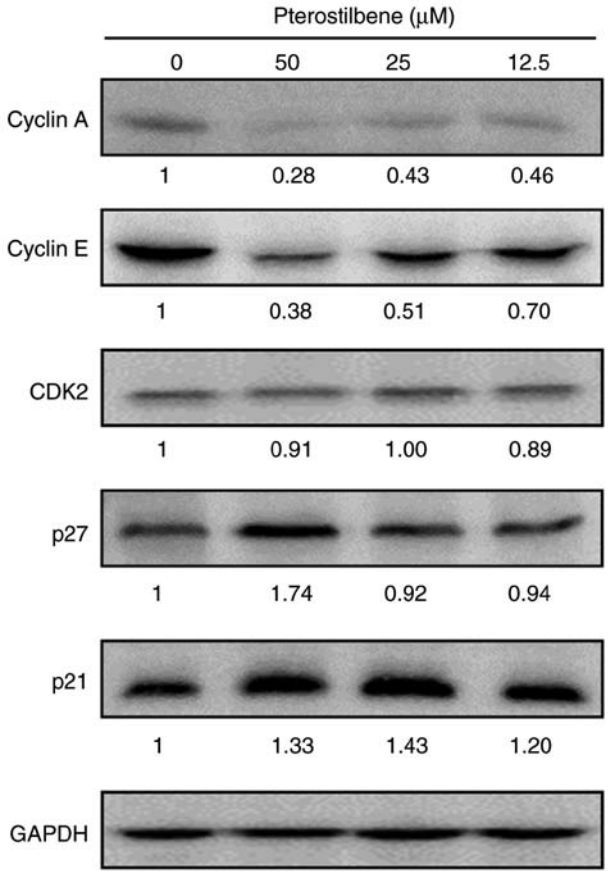

Figure 3. Effects of pterostilbene on S phase-associated regulatory proteins. The expression of S phase regulatory proteins in pterostilbene-treated H520 cells was examined by western blotting. GAPDH was used as the loading control. The fold change in the band intensity compared with that of the vehicle-treated cells is denoted under the western blots. Data are representative of three independent experiments.

weighed and the tumor volumes were measured three times a week using an electronic caliper (Mitutoyo Inc.). Tumor volume was calculated according to the following formula: (a x b^2 x0.5), where a and b indicate the tumor's long and short diameters, respectively. The dosage and route of pterostilbene injection were based on previous research (17). To evaluate the toxicity of the pterostilbene treatment on the mice, the weights of the body, heart, lung, liver, kidney and spleen were recorded.

Statistical analysis. For comparison between two groups, an unpaired two-tailed t-test (Student's t-test) was conducted. One-way or two-way ANOVA followed by Tukey's HSD post hoc test was used to compare multiple groups. Data are presented as the mean ± standard deviation. All statistical analyses were performed using GraphPad Prism version 5.0 (GraphPad Software, Inc.). $P<0.05$ was considered to indicate a statistically significant difference.

Results

Cytotoxic effect of pterostilbene on the viability of H520 tumor cells. The cytotoxic effect of pterostilbene on the viability of SqCC cancer cell lines was determined using an MTT assay. In the present study, H520 and H226 human SqCC cancer cell lines were treated with different concentrations of pterostilbene for 24 and 48 h. As illustrated in Fig. 1A, pterostilbene induced cytotoxicity in human SqCC cancer cell lines in a dose-dependent manner. Notably, these two SqCC cell lines exhibited different sensitivities to pterostilbene; the IC50 values of pterostilbene for H520 cells were 47.7±5.3 and 31.4±4.6 μM at 24 and 48 h, respectively, while the IC50 values for H226 cells were >50 and 44.3±3.7 μM at 24 and 48 h, respectively. In addition, the cell morphology and shape were assessed using an inverted microscope; this assessment indicated apoptotic morphological changes, including cell shrinkage and cytoplasmic blebbing, in the treated cells (Fig. 1B). The results demonstrated that the H520 cell line was highly sensitive to pterostilbene treatment; therefore H520 was selected for the subsequent analysis and evaluation of the cytotoxic potency of pterostilbene.

Pterostilbene induced S phase arrest and apoptosis in H520 cells. The present study subsequently investigated the impact of pterostilbene on different cell cycle phases in H520 cells. The H520 cells were exposed to different concentrations of pterostilbene for 48 h and were subjected to flow cytometric analysis following staining with PI. As Fig. 2A illustrates, the percentage of cells in S phase was markedly increased following exposure to 12.5-50 μM pterostilbene for 48 h. Additionally, the sub-G1 cell population, which is indicative of cell mortality, was increased in the presence of 50 μM pterostilbene. To confirm whether apoptotic mechanisms may have been involved in the cell death associated with treatment with pterostilbene, H520 cells were treated with pterostilbene for 48 h and subjected to flow cytometric analysis following Annexin V-FITC and PI staining. A quantitative flow cytometric analysis revealed that the percentages of early apoptotic H520 cells (Annexin V^+/PI^-, lower right quadrant) were increased by pterostilbene in a dose-dependent manner (Fig. 2B). Taken together, these results indicated that pterostilbene induced S phase arrest and early apoptosis in H520 SqCC cells.

Pterostilbene decreased S phase regulatory CDK and cyclin levels in H520 cells. To investigate the molecular mechanisms of pterostilbene in the induction of S phase arrest, the present study examined the effect of pterostilbene on the expression of key cell cycle regulators of S phase progression through western blot analysis. The Cip/Kip family members, p21 (Cip1) and p27 (Kip1), can inhibit the activity of cyclin E-CDK2 and cyclin A-CDK2 complexes. The results indicated that treatment with pterostilbene reduced the protein expression of cyclin A and cyclin E, but did not affect the expression of CDK2 (Fig. 3), as indicated by the fold change in the band intensity compared with that of the vehicle-treated cells. In addition, p21 and p27 protein expression was increased by treatment with pterostilbene (Fig. 3). These findings suggested that pterostilbene induced S phase arrest by regulating the expression of S phase cell cycle regulatory proteins in the H520 SqCC cell lines.

Pterostilbene stimulated the activity of caspase-3, -8 and -9 in H520 cells. In order to determine whether pterostilbene induced apoptotic cell death in H520 cells through the

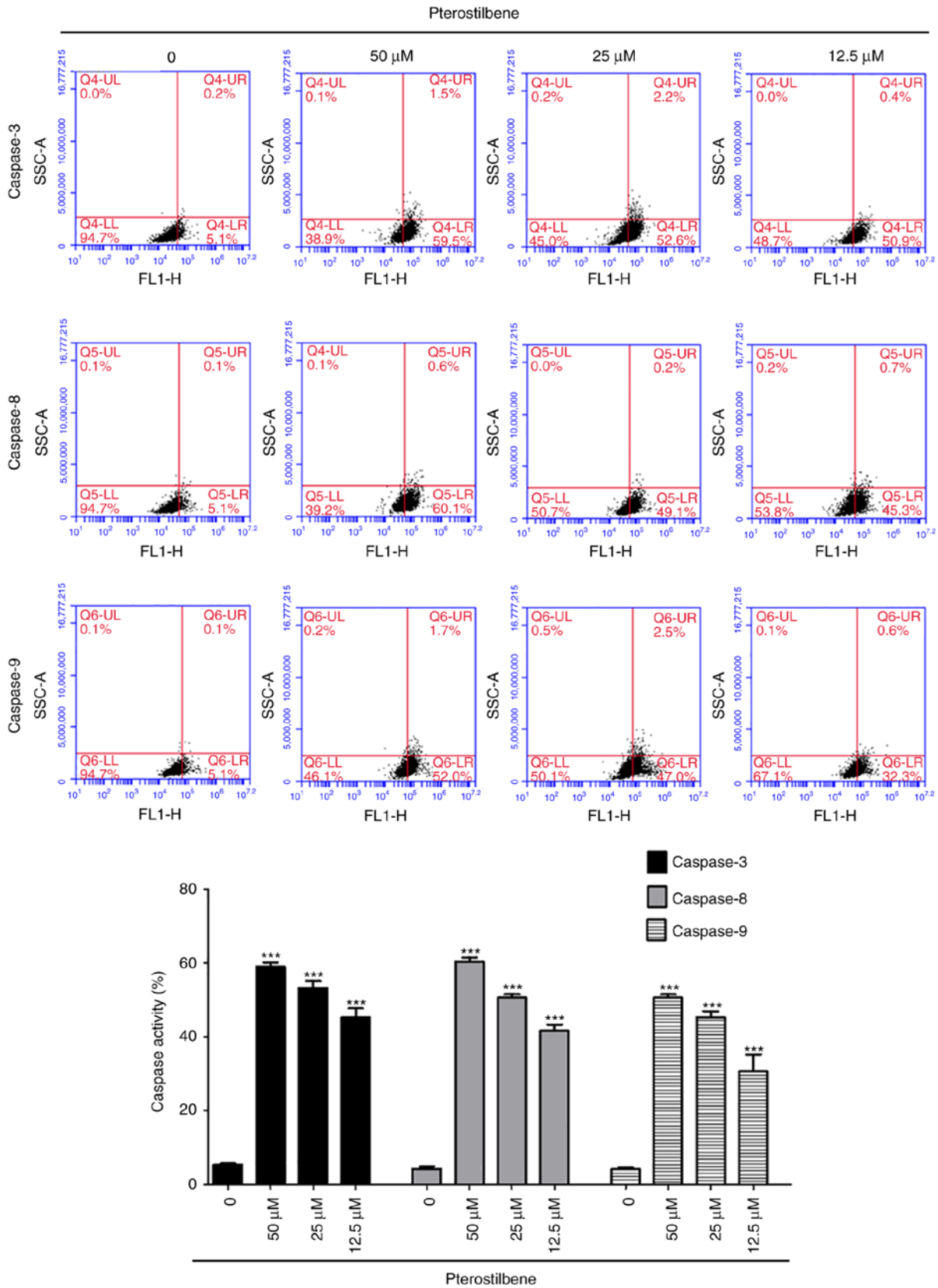

Figure 4. Effects of pterostilbene on the activity of caspase-3, -8, and -9 in H520 cells. The cells were treated with 50, 25 and 12.5 μM pterostilbene for 48 h and harvested and the caspase activity was analyzed by flow cytometry. Data are representative of three independent experiments. ***P<0.001 vs. 0.1% DMSO-treated group.

activation of caspase-3, -8 and -9, H520 cells were treated with pterostilbene for 48 h, harvested and examined using flow cytometry. Pterostilbene increased the activity of caspase-3, -8 and -9 (Fig. 4) in a dose-dependent manner and induced cell death through the activation of caspase-3, -8 and -9 in H520 cells.

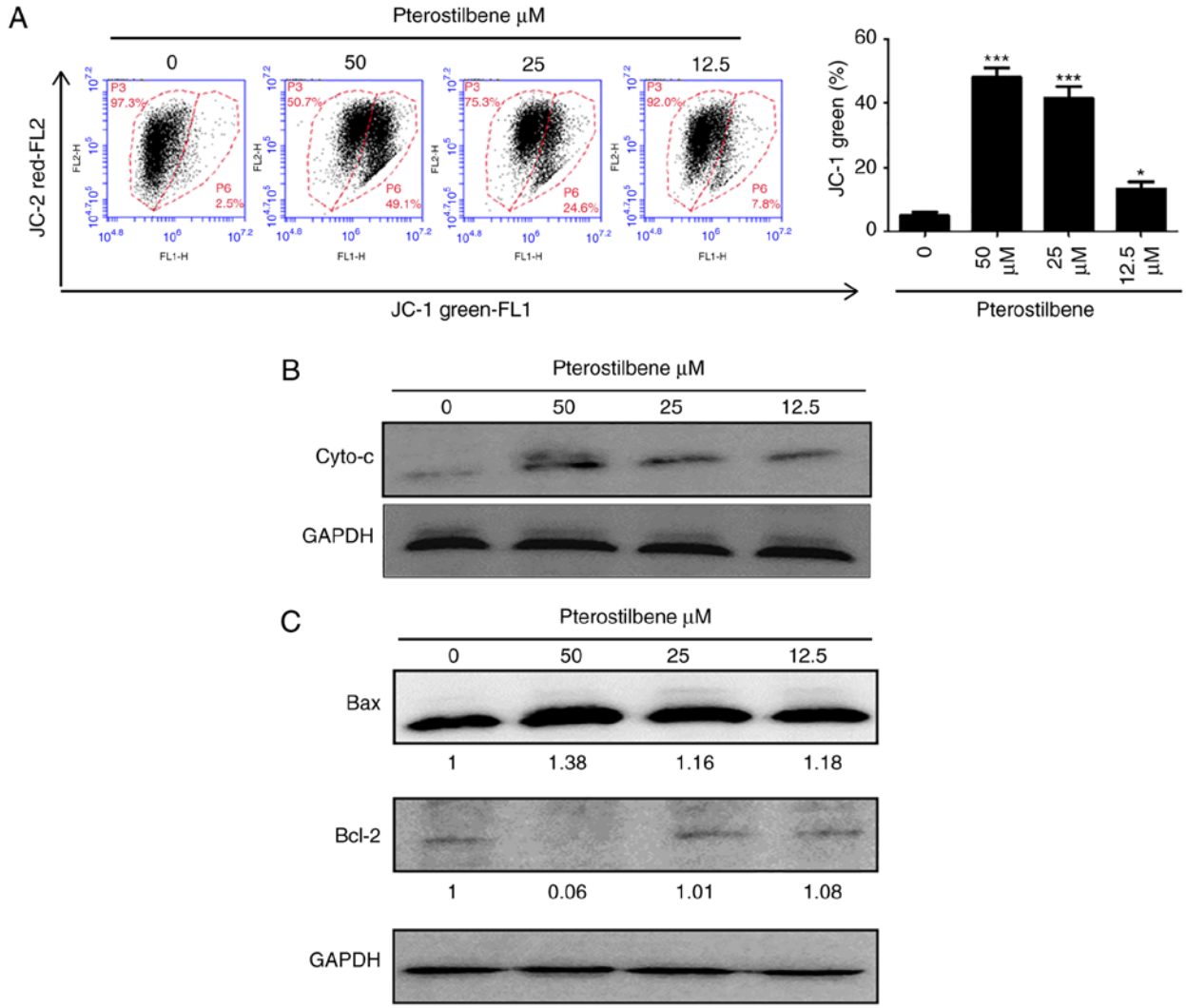

Figure 5. Effects of pterostilbene on the mitochondrial potential and cytochrome *c* release in H520 cells. Cells were treated with 50, 25 and 12.5 μM pterostilbene for 48 h. (A) Cells were stained with fluorescent JC-1 dye, and the mean JC-1 fluorescence intensity was analyzed by flow cytometry. Gate P6 was used to determine the JC-1 green percentage. (B) Cytosolic lysates were prepared, and the expression of cytochrome *c* in pterostilbene-treated H520 cells was examined by western blot analysis. (C) Total lysates were prepared, and the expression of Bax and Bcl-2 proteins in pterostilbene-treated H520 cells was examined by western blotting. The fold change in the band intensity compared with that of the vehicle-treated mice is denoted. Data are representative of three independent experimental repeats. *P<0.05 and ***P<0.001 vs. 0.1% DMSO-treated group.

Pterostilbene depolarized the mitochondrial membrane potential and increased cytochrome c release. The loss of mitochondrial membrane has a major role in the induction of apoptosis. Therefore, the membrane-permeable JC-1 dye was used to examine the mitochondrial membrane in H520 cells that has been treated with pterostilbene. As presented in sFig. 5A, following treatment with pterostilbene, a dose-dependent increase in the green fluorescence was observed in H520 cells, suggesting that pterostilbene produced significant mitochondrial depolarization. Cytochrome *c* release from the mitochondria to the cytosol is also a key initial step in apoptosis. Therefore, in order to determine whether cytochrome *c* was released during pterostilbene-induced apoptosis, western blot analysis was performed to analyze the cytochrome *c* level in the cytosolic fractions of H520 cells that had been exposed to pterostilbene. As presented in Fig. 5B, an increase in cytochrome *c* at 48 h was observed in the cytosolic fraction of the pterostilbene-treated cells, compared with the cytochrome *c* level in the control cells. In terms of the expression of Bcl-2 family members, such as the anti-apoptotic protein Bcl-2 and the pro-apoptotic protein Bax, have been identified during critical events in the mitochondrial apoptotic pathway; therefore, the present study further investigated the effects of pterostilbene on the expression of Bax and Bcl-2 in H520 cells by western blot analysis, and there was an increase in Bax protein expression and a decrease in Bcl-2 expression in H520 cells (Fig. 5C). These data suggested that pterostilbene induced the caspase-dependent mitochondrial apoptotic pathways in H520 cells.

Pterostilbene activity against H520 xenografts in nude mice. The present study then investigated whether pterostilbene had an effect against H520 xenografts in nude mice. As illustrated in Fig. 6A-C, compared with the effect of the vehicle control, pterostilbene (50 mg/kg) was able to reduce the tumor volume (Fig. 6A and B) and weight (Fig. 6C) (day 38), indicating that pterostilbene also inhibited the growth of SqCC cells *in vivo*. The toxic effect of treatment with pterostilbene was investigated in H520 xenograft models. As illustrated

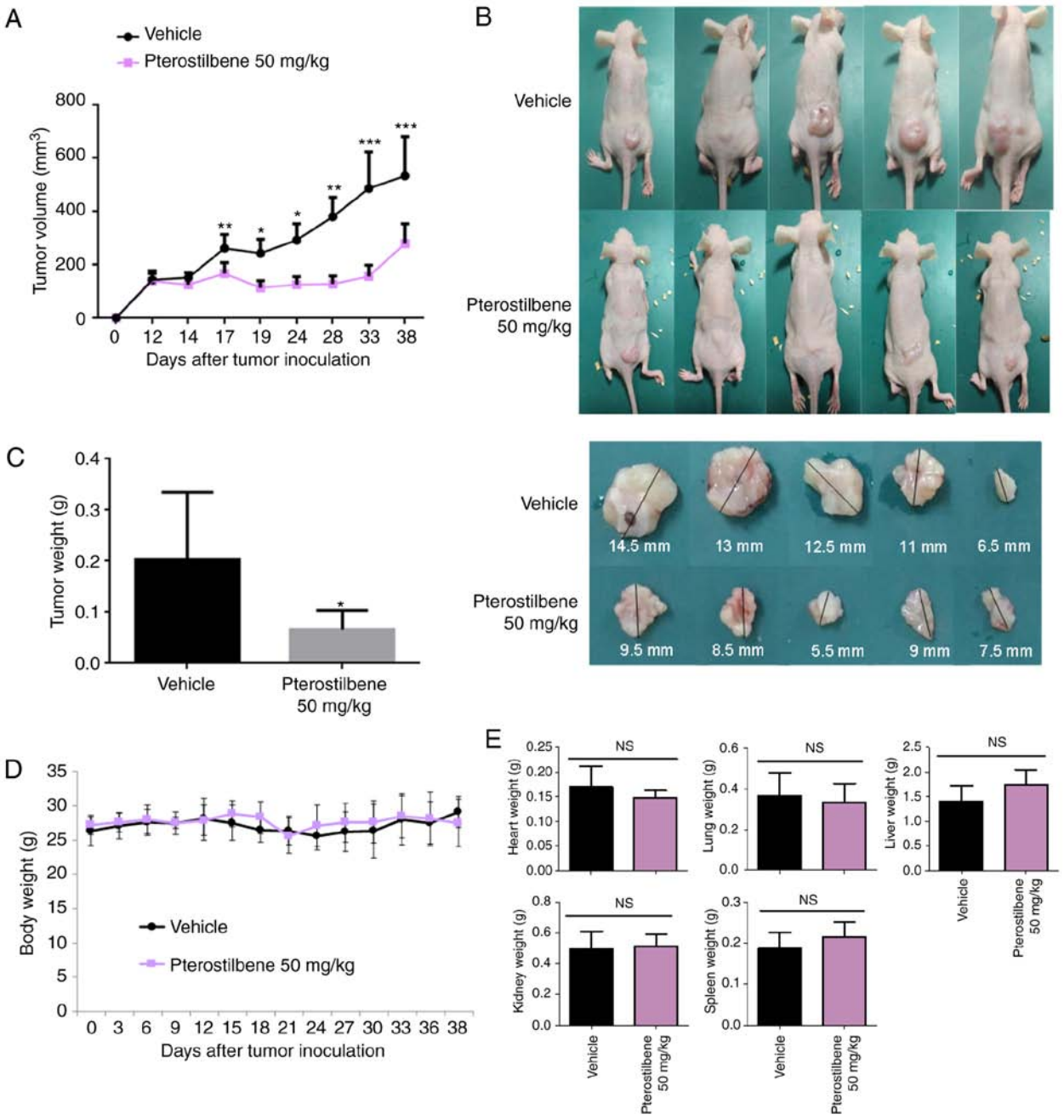

Figure 6. Effects of pterostilbene on H520 xenograft growth in nude mice. H520 cells ($1x10^7$) were inoculated under the skin of nude mice and tumors were permitted to grow to ~10 mm^3. Subsequently, pterostilbene (50 mg/kg) or vehicle control was administered intraperitoneally three times weekly until day 38 (n=6). (A) Tumor size was measured at 3-5 day intervals. *P<0.05, **P<0.01 and ***P<0.001 vs. vehicle control group (10% DMSO + 90% glyceryl trioctanoate). (B) Representative tumor images and (C) tumor weights of each group on day 38 are presented. *P<0.05 vehicle control group (10% DMSO + 90% glyceryl trioctanoate). (D) Body weight and (E) organ weight of the heart, lung, liver, kidney and spleen of pterostilbene-treated and vehicle control-treated mice. NS, not significant.

in Fig. 6D and E, there was no significant difference in body weight (Fig. 6D), or heart, lung, liver, kidney, and spleen weights (Fig. 6E) between the pterostilbene-treated group and the vehicle-treated group, which suggested that treatment with pterostilbene did not obviously exhibit adverse side effects.

Discussion

The present investigated the inhibitory effect of pterostilbene on tumor growth in the EGFR-negative lung SqCC cell line H520 and the potential signaling pathways through which pterostilbene operates. Consistent with a previous study, pterostilbene inhibited lung SqCC cell viability in a concentration- and time-dependent manner (18). The data obtained by the present study also indicated that pterostilbene promoted mortality of cancer cells through S phase cell cycle arrest and the induction of intrinsic and extrinsic apoptosis. Additionally, to the best of our knowledge, the BALB/c athymic nude mouse xenograft model experiment is the first to report the *in vivo* antitumor effect of pterostilbene in lung SqCC. Therefore, pterostilbene may be a potent therapeutic agent either alone or combined with another chemotherapeutic agent in the treatment of lung SqCC.

Lung cancer remains the leading cause of malignancy-associated mortality worldwide (1). Despite early diagnosis and advances in therapeutic strategies, outcomes have remained poor in recent decades (19). The primary cause of treatment failure is resistance to standard therapy, especially apoptosis-inducing drugs (18). Further, chemotherapy-associated side effects are major concerns. Thus, it is desirable to identify novel drugs that contain less harmful natural materials to complement and improve the efficacy of traditional chemotherapeutics. Previous studies have demonstrated that naturally occurring compounds in foods such as fruits or vegetables may exert a chemopreventive and therapeutic effect against cancers (20,21). As a natural phytoalexin present in grapes and berries, resveratrol is considered to be a potential anticancer drug due to its antioxidant, anti-inflammatory, and antiproliferative activities (22). However, its poor absorption and rapid metabolism limit the potential clinical applications of resveratrol (18). Pterostilbene, the natural dimethylated analog of resveratrol, was shown to have similar structure and function to resveratrol, but a higher bioavailability, longer half-life and lower toxicity, thus demonstrating greater potential for clinical applications (9). Although numerous studies have reported that pterostilbene exhibits the hallmarks of a valuable and well-tolerated anticancer agent, few studies have investigated its anticancer mechanisms in lung SqCC (11,23).

In agreement with recent research reporting the antitumor effect of pterostilbene on various malignant cancers (24-26), the results of the present study demonstrated that pterostilbene inhibited lung SqCC tumor growth. Although the pterostilbene mechanisms of action have not yet been completely elucidated, pterostilbene may influence multiple signaling pathways critical to cancer development. It has been reported that pterostilbene could induce cell cycle arrest and apoptosis in numerous types of cancer cells, including gastric, lung, and pancreatic cancer cells (11). The results of the present study indicated that pterostilbene induced cell cycle arrest at the S phase through apoptosis-related caspase and Bcl-2 family proteins. Western blot analysis revealed that pterostilbene increased the expression of p21 and p27, and decreased the expression of cyclin A and E. The cyclin A- and E-CDK2 complexes are the most important proteins in S phase that regulate progression to the G2/M phase. If the cyclin A or E complex is inhibited, the cell cycle is arrested in S phase, leading to the inhibition of cell proliferation and the promotion of apoptosis (27). The results of the present study also indicated that the expression levels of p21 and p27, which are CDK inhibitors that can inhibit the majority of cyclin-CDK complexes, were increased by pterostilbene (27).

Although cells can die due to non-apoptotic mechanisms, apoptosis is the principal mechanism of cancer cell death for numerous chemotherapeutic agents (28). Therefore, the induction of apoptosis is considered to be a potent therapeutic strategy for the eradication of tumors. Previous medical literature has reported that pterostilbene exerts proapoptotic activities (29,30). In order to examine this hypothesis, the present study analyzed the activity of caspase-3, -8 and -9. These caspases are the enzymes involved in the effector phase of apoptosis. Caspase-3 is the most critical component in the apoptotic pathway and can be activated by caspase-8 or caspase-9, which are the two key proteins in the extrinsic and intrinsic apoptotic pathways, respectively (31). Previously, Schneider *et al* (29) revealed that pterostilbene upregulates caspase-3/7 activity in SqCC (SK-MES-1) cell lines, suggesting a pterostilbene-induced mitochondrial mechanism of apoptosis. The results of the present study indicated that pterostilbene increased the expression of caspase-3, -8, and -9, suggesting that pterostilbene induced the apoptosis of lung SqCC cells in a caspase-dependent manner, potentially through the activation of the extrinsic and intrinsic apoptotic pathways. These results are similar to those obtained by Xie *et al* (10) who observed an increase in caspase-dependent apoptosis in multiple myeloma cells. In addition, Pan *et al* (32) also reported that pterostilbene promoted apoptosis and induced cell cycle arrest in gastric cancer AGS cells, by activating the caspase cascade and inducing changes in several cell cycle-regulating proteins, which is in agreement with the results of the current study.

To summarize, the present study demonstrated the antitumor effect of pterostilbene in lung SqCC, and revealed that pterostilbene could cause cell cycle arrest, induce apoptosis in lung SqCC cell lines *in vitro*, and inhibit tumor growth *in vivo* in a mouse xenograft model. Furthermore, recent *in vivo* safety analyses have revealed that pterostilbene does not harm mice or humans (23,33). In this regard, as it is a natural compound that exhibits low toxicity, pterostilbene may exhibit potential to treat lung SqCC in a clinical setting. Further study is required to evaluate the efficacy of pterostilbene if it is combined with different chemotherapeutic regimens or with radiation.

Acknowledgements

Not applicable.

Funding

No funding was received.

Availability of data and materials

The analyzed datasets generated during the study are available from the corresponding author upon reasonable request.

Authors' contributions

KTT, SHL and CCY conceived and designed the study. KTT, PWC, SL and TMK performed the experiments. KTT, SHL, and CCY wrote the paper. KTT, SHL, SL and CCY reviewed and edited the manuscript. All authors read and approved the manuscript and agree to be accountable for all aspects of the research in ensuring that questions about the accuracy or integrity of any part of the work are appropriately investigated and resolved.

Ethics approval and consent to participate

All animal experimental procedures were carried out following the Guide for the Care and Use of Laboratory Animals of the Institutional Animal Care and Use Committee of National Chung Hsing University (Taichung, Taiwan); the procedures were approved by the Research Ethics Committee of National Chung Hsing University.

Patient consent for publication

Not applicable.

Competing interests

The authors declare that they have no competing interests.

References

1. Siegel R, Ma J, Zou Z and Jemal A: Cancer statistics, 2014. CA Cancer J Clin 64: 9-29, 2014.
2. Okamoto T, Suzuki Y, Fujishita T, Kitahara H, Shimamatsu S, Kohno M, Morodomi Y, Kawano D and Maehara Y: The prognostic impact of the amount of tobacco smoking in non-small cell lung cancer-differences between adenocarcinoma and squamous cell carcinoma. Lung Cancer 85: 125-130, 2014.
3. Gandara DR, Hammerman PS, Sos ML, Lara PN Jr and Hirsch FR: Squamous cell lung cancer: From tumor genomics to cancer therapeutics. Clin Cancer Res 21: 2236-2243, 2015.
4. Yang CC, Fong Y, Lin LC, Que J, Ting WC, Chang CL, Wu HM, Ho CH, Wang JJ and Huang CI: The age-adjusted Charlson comorbidity index is a better predictor of survival in operated lung cancer patients than the Charlson and Elixhauser comorbidity indices. Eur J Cardiothorac Surg 53: 235-240, 2018.
5. Ettinger DS, Wood DE, Aisner DL, Akerley W, Bauman J, Chirieac LR, D'Amico TA, DeCamp MM, Dilling TJ, Dobelbower M, *et al*: Non-small cell lung cancer, version 5.2017, NCCN clinical practice guidelines in oncology. J Natl Compr Canc Netw 15: 504-535, 2017.
6. Ettinger DS, Akerley W, Borghaei H, Chang AC, Cheney RT, Chirieac LR, D'Amico TA, Demmy TL, Govindan R, Grannis FW Jr, *et al*: Non-small cell lung cancer, version 2.2013. J Natl Compr Canc Netw 11: 645-653, 2013.
7. Shi A, Zhu G, Wu H, Yu R, Li F and Xu B: Analysis of clinical and dosimetric factors associated with severe acute radiation pneumonitis in patients with locally advanced non-small cell lung cancer treated with concurrent chemotherapy and intensity-modulated radiotherapy. Radiat Oncol 5: 35, 2010.
8. Rimando AM, Kalt W, Magee JB, Dewey J and Ballington JR: Resveratrol, pterostilbene, and piceatannol in vaccinium berries. J Agric Food Chem 52: 4713-4719, 2004.
9. Estrela JM, Ortega A, Mena S, Rodriguez ML and Asensi M: Pterostilbene: Biomedical applications. Crit Rev Clin Lab Sci 50: 65-78, 2013.
10. Xie B, Xu Z, Hu L, Chen G, Wei R, Yang G, Li B, Chang G, Sun X, Wu H, *et al*: Pterostilbene inhibits human multiple myeloma cells via ERK1/2 and JNK pathway in vitro and in vivo. Int J Mol Sci 17: pii: E1927, 2016.
11. McCormack D and McFadden D: Pterostilbene and cancer: Current review. J Surg Res 173: e53-e61, 2012.
12. Prabhakar CN: Epidermal growth factor receptor in non-small cell lung cancer. Transl Lung Cancer Res 4: 110-118, 2015.
13. Tang Z, Du R, Jiang S, Wu C, Barkauskas DS, Richey J, Molter J, Lam M, Flask C, Gerson S, *et al*: Dual MET-EGFR combinatorial inhibition against T790M-EGFR-mediated erlotinib-resistant lung cancer. Br J Cancer 99: 911-922, 2008.
14. Zhang H, Zhan C, Ke J, Xue Z, Zhang A, Xu K, Shen Z, Yu L and Chen L: EGFR kinase domain mutation positive lung cancers are sensitive to intrapleural perfusion with hyperthermic chemotherapy (IPHC) complete treatment. Oncotarget 7: 3367-3378, 2016.
15. Zhang H, Li N, Chen Y, Huang LY, Wang YC, Fang G, He DC and Xiao XY: Protein profile of human lung squamous carcinoma cell line NCI-H226. Biomed Environ Sci 20: 24-32, 2007.
16. Zang JP and Wei R: Effects of Cx43 gene modification on the proliferation and migration of the human lung squamous carcinoma cell line NCI-H226. Genet Mol Res 14: 13110-13119, 2015.
17. Li K, Dias SJ, Rimando AM, Dhar S, Mizuno CS, Penman AD, Lewin JR and Levenson AS: Pterostilbene acts through metastasis-associated protein 1 to inhibit tumor growth, progression and metastasis in prostate cancer. PLoS One 8: e57542, 2013.
18. Mannal PW, Alosi JA, Schneider JG, McDonald DE and McFadden DW: Pterostilbene inhibits pancreatic cancer in vitro. J Gastrointest Surg 14: 873-879, 2010.
19. Wang BY, Huang JY, Cheng CY, Lin CH, Ko J and Liaw YP: Lung cancer and prognosis in taiwan: A population-based cancer registry. J Thorac Oncol 8: 1128-1135, 2013.
20. Siddiqui IA, Adhami VM, Ahmad N and Mukhtar H: Nanochemoprevention: Sustained release of bioactive food components for cancer prevention. Nutr Cancer 62: 883-890, 2010.
21. Riboli E, Slimani N and Kaaks R: Identifiability of food components for cancer chemoprevention. IARC Sci Publ: 23-31, 1996.
22. Suh N, Paul S, Hao X, Simi B, Xiao H, Rimando AM and Reddy BS: Pterostilbene, an active constituent of blueberries, suppresses aberrant crypt foci formation in the azoxymethane-induced colon carcinogenesis model in rats. Clin Cancer Res 13: 350-355, 2007.
23. Riche DM, McEwen CL, Riche KD, Sherman JJ, Wofford MR, Deschamp D and Griswold M: Analysis of safety from a human clinical trial with pterostilbene. J Toxicol 2013: 463595, 2013.
24. Pei HL, Mu DM and Zhang B: Anticancer activity of pterostilbene in human ovarian cancer cell lines. Med Sci Monit 23: 3192-3199, 2017.
25. Kong Y, Chen G, Xu Z, Yang G, Li B, Wu X, Xiao W, Xie B, Hu L, Sun X, *et al*: Pterostilbene induces apoptosis and cell cycle arrest in diffuse large B-cell lymphoma cells. Sci Rep 6: 37417, 2016.
26. Wawszczyk J, Kapral M, Hollek A and Weglarz L: In vitro evaluation of antiproliferative and cytotoxic properties of pterostilbene against human colon cancer cells. Acta Pol Pharm 71: 1051-1055, 2014.
27. Mann MB and Kaldis P: Cell cycle transitions and Cdk inhibition in melanoma therapy: Cyclin' through the options. Cell Cycle 10: 1349, 2011.
28. Aleo E, Henderson CJ, Fontanini A, Solazzo B and Brancolini C: Identification of new compounds that trigger apoptosome-independent caspase activation and apoptosis. Cancer Res 66: 9235-9244, 2006.
29. Schneider JG, Alosi JA, McDonald DE and McFadden DW: Pterostilbene inhibits lung cancer through induction of apoptosis. J Surg Res 161: 18-22, 2010.
30. Chen RJ, Ho CT and Wang YJ: Pterostilbene induces autophagy and apoptosis in sensitive and chemoresistant human bladder cancer cells. Mol Nutr Food Res 54: 1819-1832, 2010.
31. Aral K, Aral CA and Kapila Y: The role of caspase-8, caspase-9, and apoptosis inducing factor in periodontal disease. J Periodontol 90: 288-294, 2019.
32. Pan MH, Chang YH, Badmaev V, Nagabhushanam K and Ho CT: Pterostilbene induces apoptosis and cell cycle arrest in human gastric carcinoma cells. J Agric Food Chem 55: 7777-7785, 2007.
33. Ruiz MJ, Fernandez M, Pico Y, Mañes J, Asensi M, Carda C, Asensio G and Estrela JM: Dietary administration of high doses of pterostilbene and quercetin to mice is not toxic. J Agric Food Chem 57: 3180-3186, 2009.